

DOI: 10.5281/zenodo.11425262

# EVALUATION OF WATER FLOW BEHAVIOR IN A CONVEYANCE LINE USING ANSYS - WATERCAD SOFTWARE, HUALLAGA, HUÁNUCO, 2024

David Saldaña<sup>1</sup>, Mary Romero<sup>2</sup>, Gustavo Huerta<sup>3</sup>, Giovene Perez<sup>4</sup>

<sup>1</sup>Universidad Continental, Perú, 75085025@continental.edu.pe

<sup>2</sup>Universidad Continental, Perú, 75226509@continental.edu.pe

<sup>3</sup>Universidad Continental, Perú, 72094823@continental.edu.pe

<sup>4</sup>Universidad Continental, Perú, gperezc@continental.edu.pe

Received: 11/11/2025

Accepted: 18/12/2025

Corresponding Author: David Saldaña  
(75085025@continental.edu.pe)

## ABSTRACT

*This research aims to evaluate the behavior of water flow in the Huallaga irrigation system using the software tools ANSYS 2024 and WaterCAD 2021, with the objective of understanding the impact of water hammer in the transmission line located in the province of Huallaga, in the department of Huánuco. The study was conducted through hydraulic simulations, calculating the pressure and flow velocity along the distribution network under different flow rates. The results show that the irrigation system can handle flow rates of up to 15 L/s without the occurrence of water hammer or posing any significant risk to the system. This ensures safe and efficient operation under normal conditions. However, in scenarios involving elevated flow rates of 50 L/s, the results indicate that pressures reach critical values, which could compromise the integrity of the pipelines and other system components due to the high pressure generated by water hammer. This scenario is also linked to the potential effects of climate change, which could alter precipitation patterns and increase flow variability. The integration of climate change scenarios into the simulation models is essential to ensure that the system is resilient and capable of operating efficiently in the future, guaranteeing water supply under increasingly unpredictable climate conditions.*

---

**KEYWORDS:** Modeling, Climate Change, Water Hammer, ANSYS, WaterCAD, Huallaga River, Hydraulic Infrastructure.

---

## 1. INTRODUCTION

The Water is an essential resource for life and sustainable development, especially in the agricultural sector, which accounts for more than 70% of the available freshwater worldwide [1, 2]. In Peru, the efficient management of irrigation water is crucial, particularly in regions such as Huánuco, where water resources are fundamental for various activities, including agriculture [3, 4]. However, the increasing demand for water—driven by climate change and population growth—has intensified competition for this resource, making it imperative to improve the efficiency of irrigation systems [5]. In response to this situation, the design and analysis of water distribution systems for irrigation in Huallaga (Huánuco) require ongoing evaluation of hydraulic phenomena that affect their performance and efficiency. One such phenomenon is water hammer [6, 7], which occurs due to pressure surges and drops resulting from variations in water flow velocity within a pipeline [8, 9]. These pressure fluctuations not only impact the integrity of pipes, valves, and other components of the irrigation system, but they can also affect water quality and the overall efficiency of the distribution network [10, 11].

The Huallaga River basin presents significant altitudinal variability, which influences water quality and potentially its hydraulic behavior [12]. Irrigation practices in the region must adapt to local conditions and water availability, emphasizing efficiency in water resource use [13]. To address these challenges, the use of hydraulic modeling tools such as ANSYS and WaterCAD has proven effective in analyzing and predicting water flow behavior in complex distribution systems [14, 15]. These software tools enable the simulation of transient events, such as water hammer, and the evaluation of their impact on various system components [16]. They facilitate the optimization of design and the implementation of control measures to mitigate the adverse effects of water hammer [17].

Recent research has demonstrated the effectiveness of these software tools in the analysis of pipeline systems. For example, ANSYS Fluent stands out in the simulation of complex hydraulic phenomena through computational fluid dynamics (CFD) methods [18]. ANSYS Fluent has been used to simulate the purging process in dead-end pipelines, while Iakovlev and Morozov [19] employed it to study non-freezing conditions in large containers. Both studies highlight the usefulness of ANSYS Fluent in optimizing hydraulic systems and designing solutions adapted to extreme climate extreme variations [20].

On the other hand, WaterCAD has been consistently used in the optimization of water distribution networks. Sutharsan [21] employed this software along with WaterGEMS to analyze and optimize community water distribution systems. The results demonstrated that the optimized model not only improved water flow efficiency but also ensured a constant and reliable supply for the community, maintaining node pressures within acceptable limits.

In response to this context, the present study focuses on optimizing the design and operation of water conveyance systems for irrigation in the Huánuco region of Peru, with a specific emphasis on the phenomenon of water hammer. This hydraulic phenomenon can cause significant damage to water conveyance infrastructure, compromising the efficiency and sustainability of irrigation systems. The lack of detailed analysis regarding water flow behavior under water hammer conditions in the Huallaga transmission line represents a risk to the system's integrity and the efficient management of water resources in the region [22].

The present study aims to evaluate the behavior of water flow in the Huallaga irrigation transmission line using the ANSYS and WaterCAD software in the presence of the water hammer phenomenon, focusing on the province of Huallaga in the department of Huánuco. The objective is to apply the water hammer principle to the pipelines of the Huashga irrigation transmission line, in order to analyze and assess flow velocities along the respective sections, through the development of a hydraulic model of the line, and to perform the corresponding hydraulic calculations related to water hammer. This analysis will provide valuable information for optimizing the design and operation of the irrigation system, contributing to more efficient and sustainable water management in the region [23, 24].

This research is framed within the need to develop innovative solutions to improve irrigation efficiency and water conservation, taking into account the specific challenges of the Huánuco region and the complexities associated with the water hammer phenomenon [25, 26]. The results of this study will not only contribute to the scientific understanding of hydraulic behavior in irrigation systems but will also provide practical insights for improving the design and management of irrigation infrastructure in the region, promoting a more sustainable use of water in local agriculture [27, 28]. There is limited research on the simulation of water hammer using implicit finite difference methods, where solving the basic equations of transient flow requires resolving a

system of equations [29].

## 2. MATERIALS AND METHODS

### 2.1. Study Area

The political location of the study area is in the Department of Huánuco, Province of Huacaybamba, and District of Huacaybamba. The populated centers included in this area are Huashga, Neocolca, and Yupan. The altitude ranges between 2,113 and 2,231 meters above sea level. The geographic coordinates of the area are 9003482.34 S and 277446.57 E [30].

Regarding the hydrographic location, the area belongs to the Pacific Ocean watershed and is situated within the Upper Huallaga River basin. The micro-watersheds that drain the area correspond to the Yupan River [31].



Figure 1: Political Map of the Huallaga Basin.

## 3. THEORETICAL FRAMEWORK

The water hammer phenomenon is a critical aspect in the design and operation of water conveyance systems [32]. This phenomenon manifests as a variation in pressure along the flow line, occurring in both gravity-driven and pressurized pumping systems [33].

### 3.1. Energy Equation

Bernoulli's Principle and Water Hammer: Water hammer can be understood as an application of Bernoulli's principle, taking into account the additional overpressure generated [34]. The equation that describes this phenomenon is:

$$\frac{v^2}{2g} + z + \frac{P}{\gamma} - h_f + \Delta P_{\text{productogolpe}} \text{-----} (1)$$

Where H is the pressure in the pipe, and the following terms are typically associated with it:  $v^2/2g$  is the kinetic head,  $z$  is the potential head,  $P/\gamma$  is the pressure head of the fluid, and  $-h_f$  represents

the head losses due to friction. Finally, the  $\Delta P$  factor caused by the water hammer results from the sudden stop, which is due to the inertia of the fluid.

### 3.2. Celerity

This is the propagation speed of the pressure wave and is a crucial parameter in water hammer analysis. It can be calculated based on the pipe's diameter and thickness, as well as the material's modulus of elasticity [35], as shown in the following equation

$$\alpha = \frac{9900}{\sqrt{48.3 + K \cdot \frac{D}{e}}} \text{-----} (2)$$

Where  $\alpha$  is the wave celerity (in m/s),  $D$  is the pipe diameter (in mm),  $e$  is the pipe wall thickness (in mm), and  $K$  is the modulus of elasticity (in  $\text{kg/m}^2$ ) of the different pipe materials.

### 3.3. Overpressures

The overpressures generated by water hammer can have significant effects on hydraulic systems [36]. These exhibit a reduction rate characterized by an initial rapid decrease followed by a gradual decay as the pipe length increases [37]. Factors such as the use of rubber bypass pipes can significantly reduce the celerity and increase the characteristic time of the phenomenon, affecting the damping rate [38]. To calculate overpressures, different formulas are used depending on the system's closure speed [39].

Michaud's Formula, used for slow closures, estimates the overpressure based on the pipe length and the change in fluid velocity. It is represented as

$$\Delta H = \frac{2 \cdot L \cdot v}{g \cdot T} \text{-----} (3)$$

Where  $\Delta H$  is the overpressure, expressed in meters of water column;  $L$  is the length (distance),  $v$  is the velocity,  $g$  is the gravitational acceleration, and  $T$  is the closure time.

Allievi's Formula, used for rapid closures where the overpressure is constant and independent of the pipe length. It is represented by

$$\Delta H = \frac{a \cdot v}{g} \text{-----} (4)$$

Where  $\Delta H$  is the overpressure,  $a$  is the wave speed (celerity),  $v$  is the velocity, and  $g$  is the gravitational acceleration.

### 3.4. Research Development

This research applies the water hammer theorem to the conveyance line of the Huallaga irrigation system, located in the department of Huánuco. To meet the stated objectives, a rigorous methodology was followed, structured in several stages.

First, data were collected through technical

datasheets and topographic surveys, recording accelerations, velocities, physical characteristics of the system (lengths, diameters, materials), and flow rates at different points. This information was essential for understanding the flow behavior. Subsequently, the Michaud and Allievi formulas were applied to calculate overpressures and depressions in different sections, identifying critical zones at risk of water hammer.

The system was modeled in WaterCAD, incorporating all collected data. Steady-state and transient simulations were performed to assess pressures, velocities, and flow rates. The results were compared with manual calculations based on the water hammer theorem, allowing validation of the model's accuracy. Next, a detailed model was built in ANSYS, where computational fluid dynamics (CFD) was applied to simulate the behavior of flow and pressure in the system's most vulnerable points.

As an illustration, Figure 2 summarizes the results for a flow rate of 15 l/s across 18 sections. A constant velocity of 1.7 m/s was observed, while pressures

ranged from -0.107 atm in the initial section to -4.066 atm in the final section, indicating a progressive pressure drop along the pipeline, highlighting critical conditions in the terminal sections.

Based on these results, the most vulnerable points to water hammer were identified, and solutions such as relief valves, air chambers, or redesign of specific sections were proposed. The effectiveness of these measures was evaluated through additional simulations in both WaterCAD and ANSYS.

This comprehensive approach, combining analytical calculations and advanced computational modeling, enables an accurate assessment of the system's behavior under water hammer conditions and supports the feasibility of the proposed solutions to mitigate its effects.

#### 4. RESULTS

The pressure results as a function of distance for flow rates of 10 l/s, 15 l/s, and 50 l/s are presented in the following graphs.

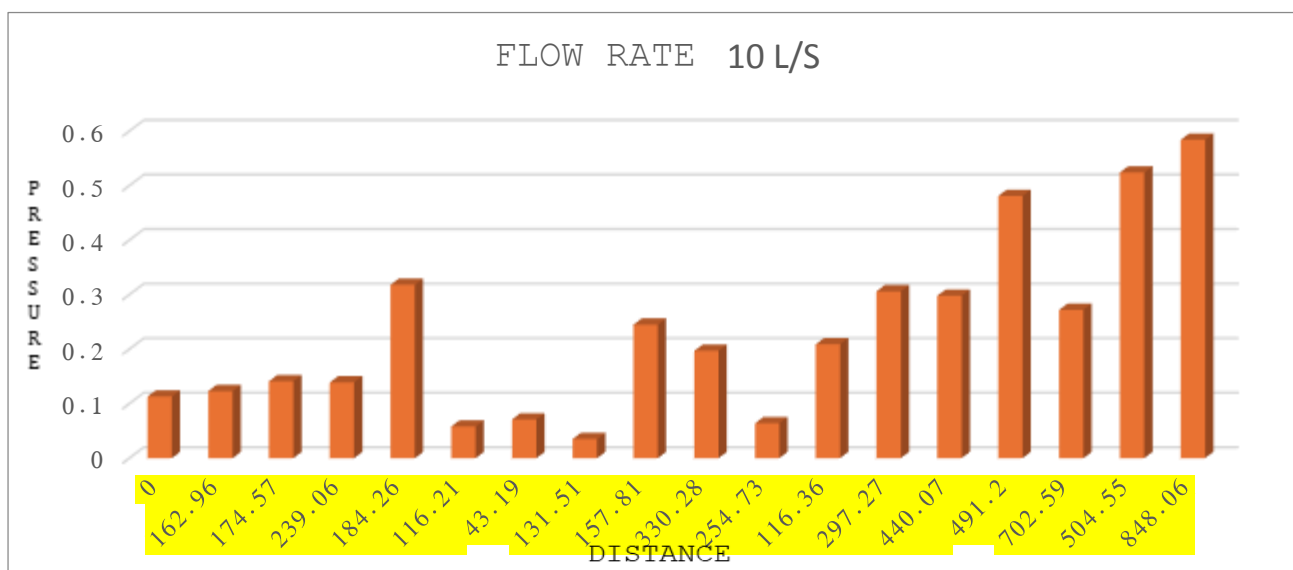


Figure 2: Pressure versus Distance along the Conveyance Line with a Flow Rate of 10 l/s (0.01 m<sup>3</sup>/s) using WaterCAD Software.

Figure 2 shows the variation of pressure as a function of distance along a conveyance line with a constant flow rate of 10 liters per second (L/s). Throughout the section, pressures fluctuate irregularly. The lowest values are recorded within the first 200 meters, with a minimum of 0.035 atm at a distance of 157.81 m. Low pressures are also observed at 43.19 m, 116.36 m, and 131.51 m, possibly due to head losses or topographic elevations. From 440 m onward, the pressure increases steadily, reaching 0.524 atm at 848.06 m and a maximum of

0.584 atm at 804.56 m. This figure helps identify the pressure behavior along the system and detect critical zones that may require adjustments to ensure efficient and safe flow.

Figure 3 shows the variation in pressure as a function of distance along a conveyance line for a flow rate of 15 liters per second (L/s). Unlike the behavior observed with a flow rate of 10 L/s, in this case all recorded pressures are negative, indicating a sub-atmospheric pressure regime throughout the entire section. This condition intensifies

progressively from 440 meters onward, where a sharp drop is observed, reaching minimum values close to -4.5 units at 848.06 m. This behavior suggests that the increased flow rate causes a greater pressure loss, possibly due to increased internal friction, adverse topographic conditions, or insufficient pipe

diameter to handle the flow. Overall, the graph highlights critical zones of hydraulic depression that could compromise the stability of the system and may require technical adjustments in the design or materials of the infrastructure.

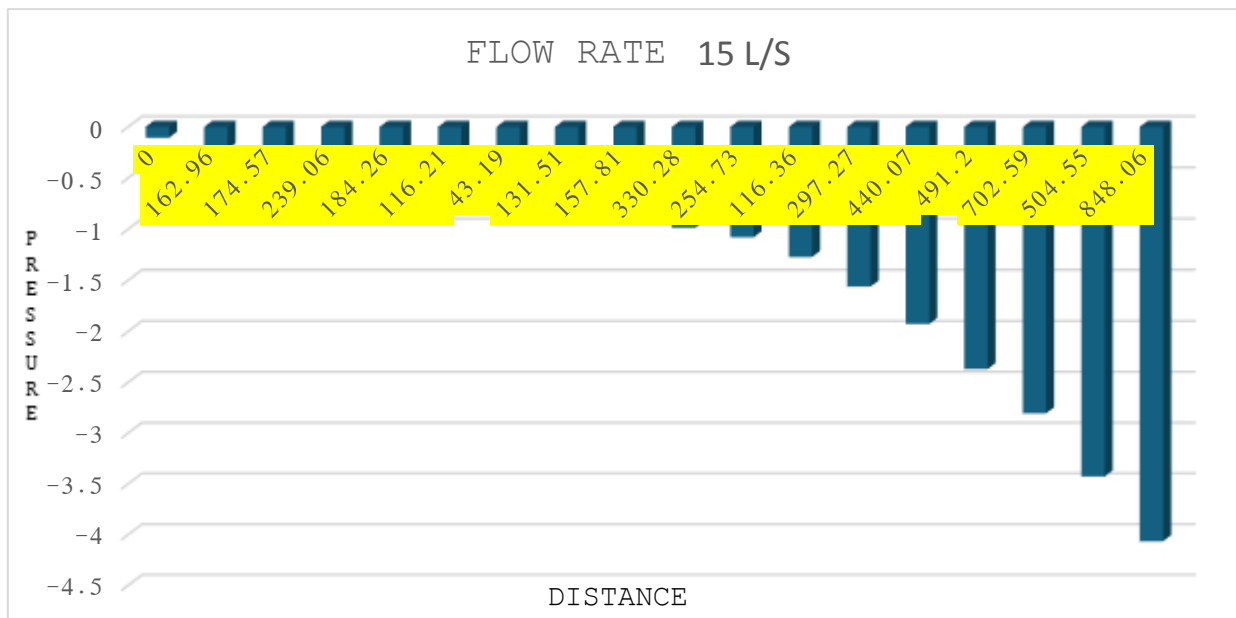


Figure 3: Pressure Versus Distance Along the Conveyance Line With a Flow Rate of 15 L/s (0.015 m³/s) Using WaterCAD Software.

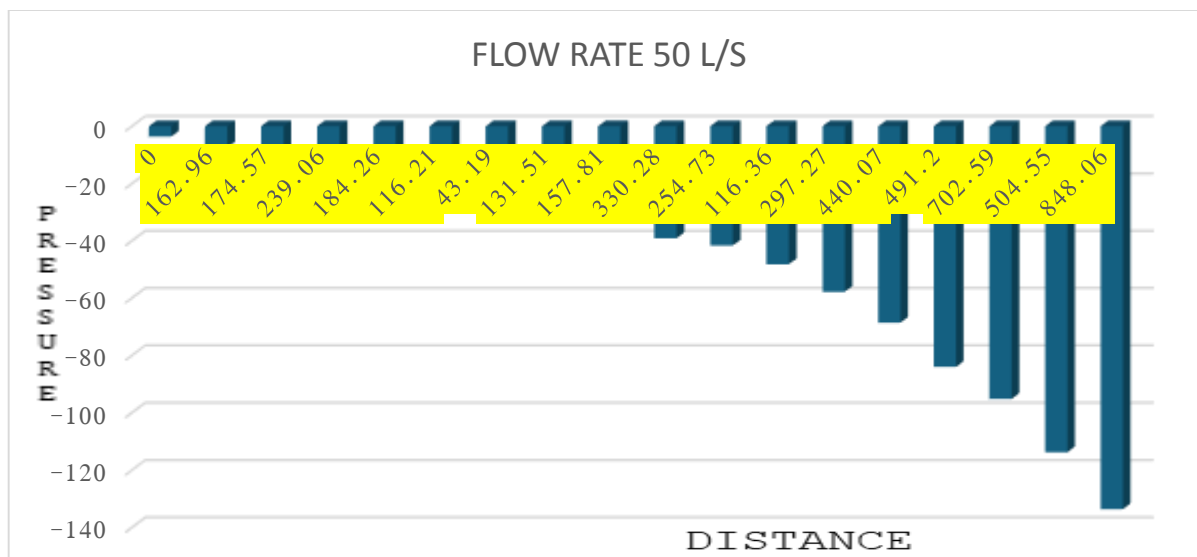


Figure 4: Pressure versus Distance along the Conveyance Line with a Flow Rate of 50 l/s (0.05 m³/s) using WaterCAD Software.

Figure 4 presents the pressure values recorded at different distances along a pipeline carrying a constant flow of 50 L/s. A progressive decrease in pressure is observed, suggesting a significant pressure loss along the route, possibly due to internal friction within the pipe or changes in terrain

elevation. The lowest recorded pressure is -133.639 atm at a distance of 904.56 meters. This behavior indicates a pressure gradient that may require intervention through the hydraulic system to prevent negative pressure conditions that could affect system performance or cause cavitation.

#### 4.1. Comparison 1: Velocity at Flow Rates of 10 l/s and 15 l/s.

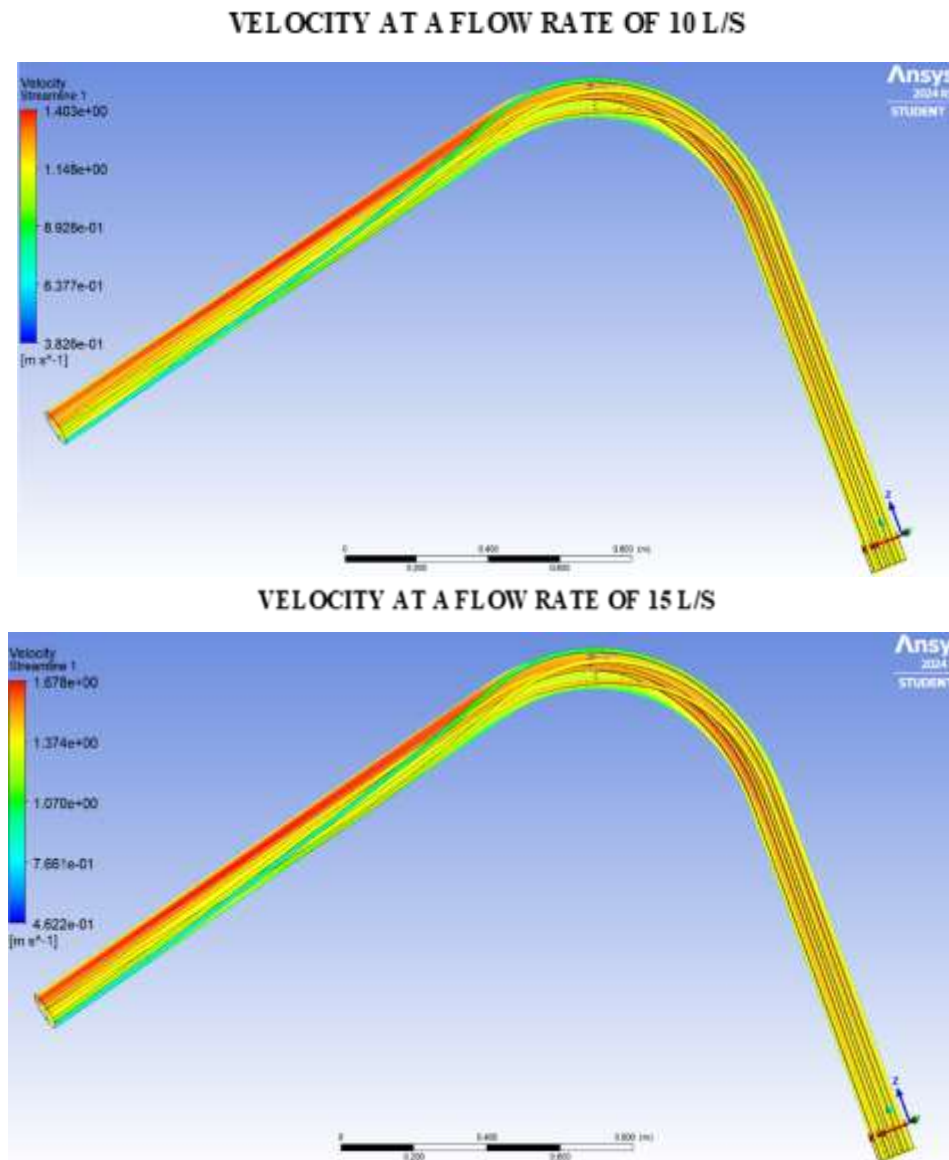


Figure 5: It Is Observed How the Flow Rate and Speed of the Fluid Are Distributed and Vary Within the Hydraulic System Created With the ANSYS Program.

The flow analysis in a 4" elbow, shown in Figure 5, demonstrates how flow rate changes affect velocity in areas where the direction is altered. With a flow rate of 10 L/s, the velocity remains constant at 1.13 m/s, while at 15 L/s, it increases to 1.7 m/s. The velocity variation begins 0.40 m from the elbow's inlet and extends approximately 2 m downstream, until the flow stabilizes.

This behavior highlights the influence of elbows on flow dynamics, affecting hydraulic stability and generating energy losses. Therefore, it is essential to consider these effects in pipeline design to optimize system performance and reduce potential disturbances.

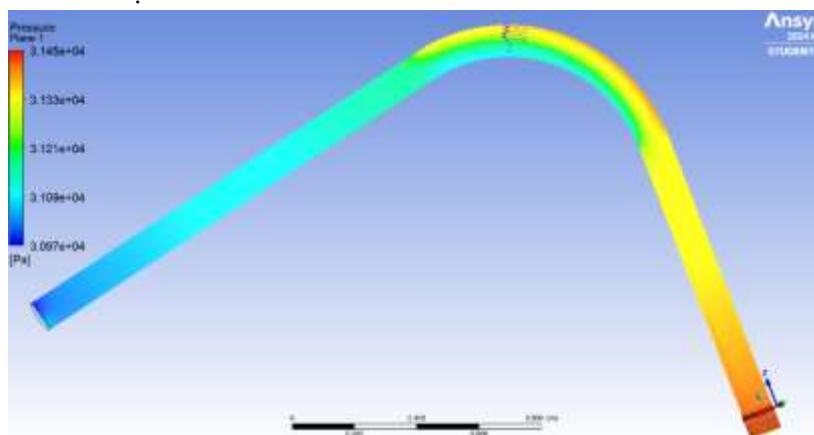
#### 4.2. Comparison 1: Pressure at Flow Rates of 10 l/s and 15 l/s

The flow analysis in Figure 6 focuses on how hydraulic conditions are affected under a specific operating scenario. Using the ANSYS software, the behavior of the flow was studied in the critical areas of the pipeline. It was observed that, for a flow rate of 10 L/s, pressure gradually decreases along the pipe and reaches a steady state after 2.50 meters. In the case of a 15 L/s flow rate, a more pronounced pressure drop is recorded, with a reduction of approximately 1.00 meter, stabilizing afterward. This analysis shows a slight increase in pressure in the

impact zone at the pipe elbow, which is characteristic of the hydraulic shock caused by the change in flow

direction. This behavior highlights the influence of elbows on pressure distribution.

**PRESSURE AT A FLOW RATE OF DE 10 L/S**



**PRESSURE AT A FLOW RATE OF DE 15 L/S**

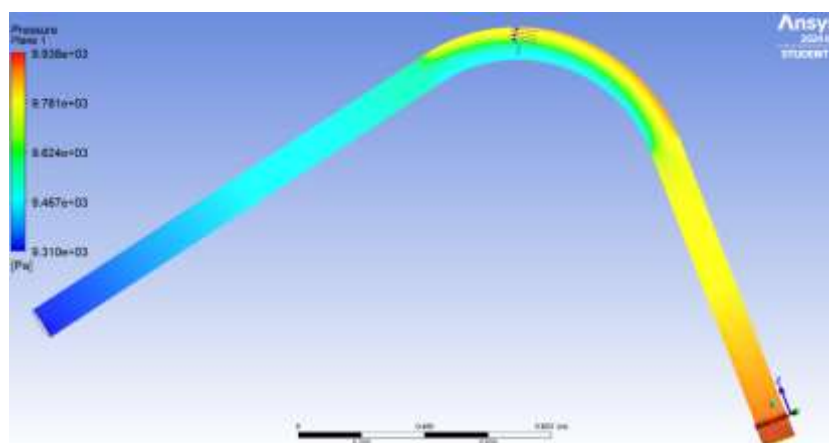


*Figure 6: It Is Observed How the Pressures and Flow Rates of the Fluid Are Distributed and Vary Within the Hydraulic System Prepared With the ANSYS Program.*

**4.3. Comparison 2: Velocity at Flow Rates of 10 l/s and 50 l/s**

Figure 7 analyzes flow rates of 10 L/s and 50 L/s, highlighting velocity changes at the inlet, outlet, and during flow stabilization. For a flow rate of 10 L/s, the velocity remains constant at 1.13 m/s, while with a flow rate of 50 L/s, the velocity is also constant, reaching 5.67 m/s.

In both cases, a variation in velocity is observed at the point where the flow direction changes (4" elbow). For the 50 L/s flow, this variation begins 0.40 m from the elbow's entrance, reaches its peak at the outlet, and extends for approximately 3.00 m before stabilizing. This behavior highlights the stresses caused by the change in direction, followed by a progressive recovery of uniform flow along the

rest of the pipeline.

The pressure analysis shown in Figure 8 evaluates how flow conditions vary in a pipe elbow under different flow rates, specifically 10 L/s and 50 L/s. With a flow rate of 10 L/s, the pressure gradually decreases along the conduit, fully stabilizing at 2.50 m, indicating a stable flow without significant disturbances.

In contrast, when the flow rate increases to 50 L/s, the pressure drops sharply, reaching negative values within the first 0.90 m before stabilizing. This behavior reveals a significant pressure increase at the elbow caused by hydraulic shock. As the flow rate rises, dynamic friction and stress intensify, indicating the presence of water hammer. This phenomenon varies in intensity: it is mild with low flow rates and critical with high flow rates.

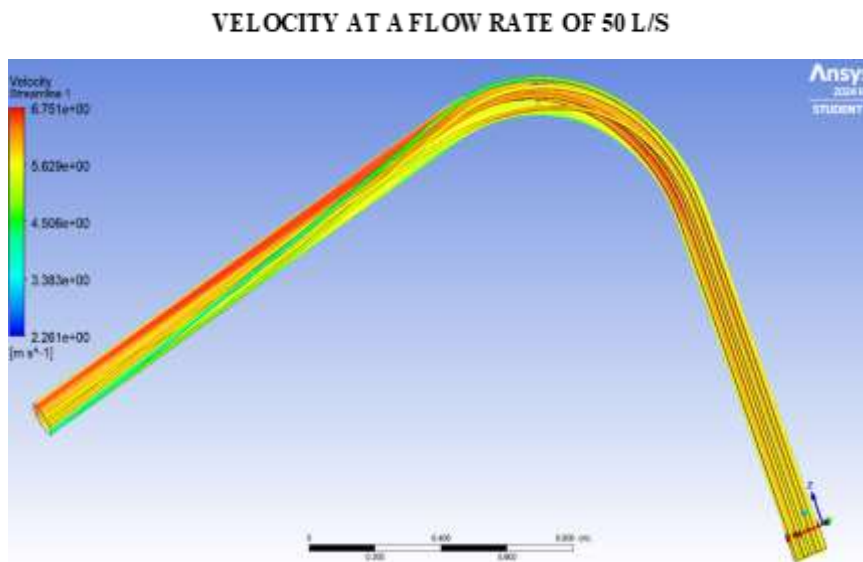
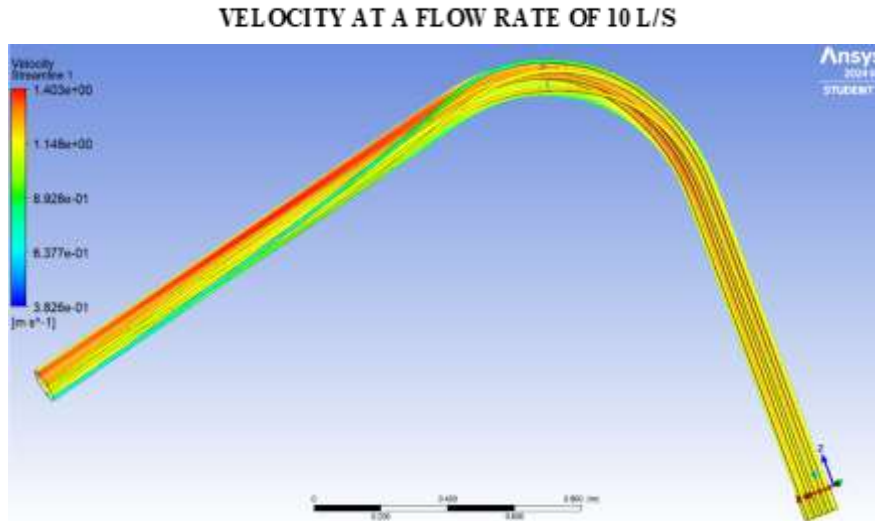
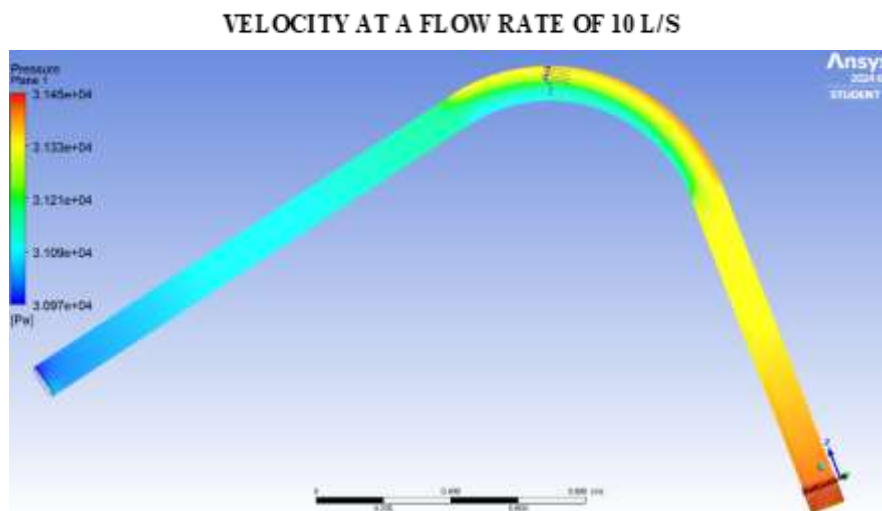


Figure 7: It Is Observed How the Flow Rate and Speed of the Fluid Are Distributed and Vary Within the Hydraulic System Created With the ANSYS Program.

**4.4. Comparison 2: Pressure at Flow Rates of 10 l/s and 50 l/s**



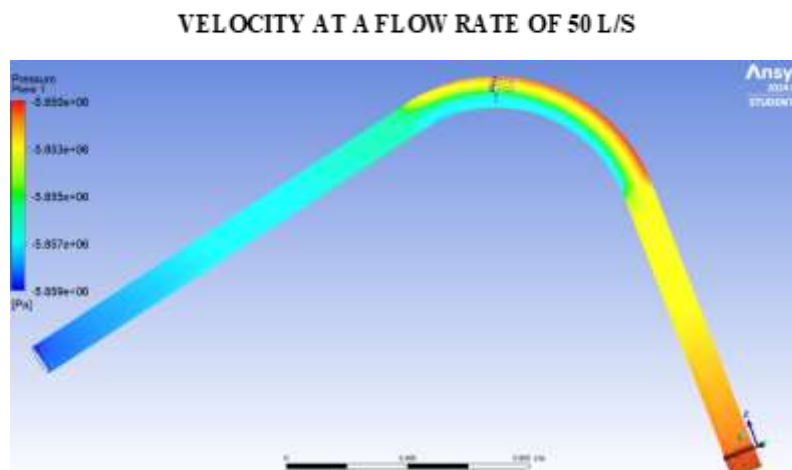


Figure 8: It Is Observed How the Pressures and Flow Rates of the Fluid Are Distributed and Vary Within the Hydraulic System Prepared With the ANSYS Program.

### 5. DISCUSSION

According to the results obtained, it was demonstrated that the water hammer phenomenon can be controlled under normal operating conditions for flow rates of 10 L/s and 15 L/s. For a flow rate of 10 L/s, a constant velocity of 1.13 m/s was recorded, with stable pressures ranging between 0.58 atm and 0.035 atm. In the case of 15 L/s, the velocity increased to 1.70 m/s, while the pressures fluctuated between -0.107 atm and -4.066 atm, stabilizing after the first meter of the pipeline.

Additionally, a projected scenario with a flow rate of 50 L/s was considered, in the context of potential climate change effects, which could require operating the system under fully filled pipe conditions. In this case, the velocity reached 5.67 m/s, and critical pressures between -3.569 atm and -133.639 atm were recorded, highlighting the need to implement protective measures against such events.

The results obtained are consistent with various previous studies. For example, in the study by [40], using a flow rate of 20 L/s with the WANDA software, a velocity of 1.30 m/s and a pressure of 0.72 atm were achieved, confirming that water hammer can be mitigated under such conditions. Similarly, in the study by [41], using ANSYS with a flow rate of 5 L/s, a velocity of 1.99 m/s and a pressure of 0.22 atm were reached, demonstrating that low flow rates contribute to controlling the phenomenon in hydraulic conduits.

The results also align with those of [42], where, through the use of WaterCAD software and a flow rate of 25 L/s, a velocity of 2.55 m/s and a pressure of 0.36 atm were obtained, confirming that moderate flow rates allow for effective management of water hammer in water supply networks.

On the other hand, the findings differ from those of [43], where flow rates of 15 L/s and 25 L/s were used, resulting in velocities of 3.11 m/s and 3.66 m/s, respectively, without successfully mitigating water hammer in an irrigation pipeline. Similarly, the results contrast with those of [44], who analyzed a flow rate of 70 L/s in an irrigation area under climate change scenarios, recording a velocity of 9.27 m/s. These results indicate that under high-flow conditions, mitigating water hammer becomes more complex and requires additional interventions.

### 6. CONCLUSION

The Huallaga irrigation system demonstrates favorable hydraulic behavior against water hammer for flow rates of 10 L/s and 15 L/s, operating within safe pressure and velocity ranges. This performance indicates the system's adequate capacity under normal and moderate operating conditions. However, when simulating high flow rates of up to 50 L/s—as might occur due to climate change and hydrological variability—critical pressures and velocities emerge that compromise the infrastructure's integrity, making the implementation of mitigation measures essential, such as relief valves, air chambers, automatic control systems, or redesigning vulnerable sections.

In this regard, the study confirms that water hammer can be effectively controlled under standard conditions, but also highlights the system's vulnerability to extreme events. The implications of these findings are significant not only for irrigation systems, but also for potable water networks and industrial facilities operating under variable flow regimes.

It is recommended that current hydraulic

engineering projects incorporate resilience criteria to extreme hydrological events from the design stage, taking into account climate change projections and variations in water demand. Additionally, the implementation of real-time monitoring systems, preventive maintenance, and advanced hydraulic

modeling is suggested as tools to optimize operation and reduce risks. Future research should focus on strategies for adapting existing infrastructure as well as on developing sustainable and scalable solutions to address the challenges posed by increasing climate uncertainty in hydraulic systems.

## REFERENCES

- FAO, *Water and One Health*. FAO, 2017. Available: <https://www.fao.org/one-health/areas-of-work/water/en>
- K. Tariq, "Chart: Globally, 70% of freshwater is used for agriculture," *The World Bank*, 2017. Available: <https://blogs.worldbank.org/en/opendata/chart-globally-70-freshwater-used-agriculture>
- OECD, *Water Governance in Peru*. OECD, 2021. Available: [https://www.oecd.org/en/publications/2021/03/water-governance-in-peru\\_0980e96a.html](https://www.oecd.org/en/publications/2021/03/water-governance-in-peru_0980e96a.html)
- Autoridad Nacional del Agua (ANA), *Política y Estrategia Nacional de Recursos Hídricos*. ANA, 2015. Available: [https://www.ana.gob.pe/sites/default/files/default\\_images/politica\\_y\\_estrategia\\_nacional\\_de\\_recursos\\_hidricos\\_ana.pdf](https://www.ana.gob.pe/sites/default/files/default_images/politica_y_estrategia_nacional_de_recursos_hidricos_ana.pdf)
- W. Asvapoositkul, T. Nimitpaitoon, S. Rattanasuwan, and P. Manakitsirisuthi, "The use of hydraulic ram pump for increasing pump head – technical feasibility," *Engineering Reports*, vol. 3, no. 5, 2021. <https://doi.org/10.1002/eng2.12314>
- G. Clark and D. Haman, "Water hammer in irrigation systems," *EDIS*, vol. 2022, no. 1, 2022. <https://doi.org/10.32473/edis-ae066-1994>
- A. Tijsseling and A. Anderson, "Johannes von Kries and the history of water hammer," *Journal of Hydraulic Engineering*, vol. 133, no. 1, pp. 1–29, 2007. [https://doi.org/10.1061/\(ASCE\)0733-9429\(2007\)133:1\(1\)](https://doi.org/10.1061/(ASCE)0733-9429(2007)133:1(1))
- I. Karim, R. Sahib, H. Abdullah, and R. Aziz, "Water hammer analysis in the main pipeline for the proposed Taq-Taq Dam irrigation project in Iraq," *IOP Conference Series: Materials Science and Engineering*, vol. 737, no. 1, art. 012154, 2020. <https://doi.org/10.1088/1757-899X/737/1/012154>
- M. Hamad, A. Hassan, and A. Abdullah, "Water hammer analysis in water pipelines and methods for protection," *Malaysian Journal of Applied Sciences*, vol. 8, no. 1, pp. 95–108, 2023. <https://doi.org/10.37231/myjas.2023.8.1.355>
- M. Jorge, Q. Mayer, A. Ariel, H. Carlos, and C. Mirna, "Estaciones de bombeo, anti-golpe de ariete y control de fugas, válvulas y sistemas automáticos," *Ibero-American Journal of Engineering & Technology Studies*, vol. 3, no. 1, pp. 433–439, 2023. <https://doi.org/10.56183/iberotecs.v3i1.617>
- S. Lupa, M. Gagnon, M. Martin, G. Sebastian, and X. Georges, "The impact of water hammer on hydraulic power units," *Energies*, vol. 15, no. 4, art. 1526, 2022. <https://doi.org/10.3390/en15041526>
- Autoridad Nacional del Agua, *Evaluación de Recursos Hídricos en la Cuenca de Huallaga*. ANA, 2015. Available: [https://repositorio.ana.gob.pe/bitstream/handle/20.500.12543/19/ANA0000049\\_1.pdf](https://repositorio.ana.gob.pe/bitstream/handle/20.500.12543/19/ANA0000049_1.pdf)
- P. Percy and R. Jose, *Crisis Alimentaria y Cambio Climático en Huánuco*. Centro de Estudios de Cambio Climático y Desarrollo Sostenible, 2023. Available: <https://www.ceccds.gob.pe>
- G. Esteban and B. Esteban, "Sistemas de información geográfica y modelado hidráulico de redes de abastecimiento de agua potable," *Revista Geográfica de América Central*, vol. 2, no. 63, pp. 293–318, 2019. <http://dx.doi.org/10.15359/rgac.63-2.11>
- S. Shibli, "Pipe network design and analysis: An example with WaterCAD," vol. 1, no. 1, pp. 1–10, 2021. <https://doi.org/10.31224/osf.io/c3aky>
- S. Shibli, "A short review on computational hydraulics in the context of water resources engineering," *Open Journal of Modelling and Simulation*, vol. 10, no. 1, pp. 1–31, 2022. <https://doi.org/10.4236/ojmsi.2022.101001>
- K. Karim, E. Mohamed, and F. Mohamed, "Experimental study on reducing water hammer effects in uPVC pipes using rubber bypass tubes," *Ain Shams Engineering Journal*, vol. 15, no. 3, art. 102562, 2024. <https://doi.org/10.1016/j.asej.2023.102562>
- F. Mohamed and E. Mohamed, "CFD simulation of purging process for dead-ends in water intermittent distribution systems," *Ain Shams Engineering Journal*, vol. 12, no. 1, pp. 167–179, 2021. <https://doi.org/10.1016/j.asej.2020.06.013>
- L. Iakovlev and I. Morozov, "Evaluation of liquid non-freezing conditions in large vessels using Ansys Fluent," *Energy Systems*, vol. 7, no. 4, pp. 18–28, 2022. <https://doi.org/10.34031/es.2022.4.002>

- D. Luis, *Sistemas de Información Geográfica y Modelado Hidráulico*. Universidad Politécnica de Madrid, 2016. Available: [https://oa.upm.es/47337/1/TFG\\_Luis\\_Felipe\\_Duran\\_Vinuesa.pdf](https://oa.upm.es/47337/1/TFG_Luis_Felipe_Duran_Vinuesa.pdf)
- M. Sutharsan, "Optimizing the water distribution network of community water supply," *Journal of Science of the University of Kelaniya*, vol. 16, no. 1, pp. 1–14, 2023. <https://doi.org/10.4038/josuk.v16i1.8070>
- P. Dionisio, H. Arthur, and P. Chris, "Irrigation technology and water conservation," *Review of Environmental Economics and Policy*, vol. 14, no. 2, pp. 216–239, 2020. <https://doi.org/10.1093/reep/reaa004>
- F. Alisher, G. Aziza, and H. Jasur, "Improvement of water accounting for irrigation systems," *IOP Conference Series: Materials Science and Engineering*, vol. 1030, no. 1, art. 012145, 2021. <https://doi.org/10.1088/1757-899X/1030/1/012145>
- K. P. Karsten, B. Susan, and B. Malene, "Hydrosocial communities and water governance in Peru," *Water International*, vol. 45, no. 3, pp. 169–188, 2020. <https://doi.org/10.1080/02508060.2020.1755538>
- W. Xiaolu *et al.*, "Hydrologic analysis of an intensively irrigated area in southern Peru," *Water*, vol. 13, no. 3, art. 318, 2021. <https://doi.org/10.3390/w13030318>
- Gobierno Regional de Huánuco, *Reparación de Bocotoma y Línea de Conducción*. Expediente No. 1122098, Perú, 2019.
- G. Ávila *et al.*, "Evolución histórica de las fuentes energéticas empleadas en el abasto de agua," *Revista Ingeniería Agrícola*, vol. 11, no. 1, pp. 47–57, 2021. Available: <https://www.redalyc.org/articulo.oa?id=586269368008>
- C. Eduardo *et al.*, "Modelamiento de un sistema de control predictivo aplicado al canal de regadío," *LACCEI Proceedings*, vol. 2, no. 6, art. 4, 2023. <https://doi.org/10.18687/LACCEI2023.1.1.1239>
- O. Mery, M. Hassan, and L. Ekaid, "Water hammer mitigation by air vessel and bypass configuration," *IOP Conference Series: Materials Science and Engineering*, vol. 1094, no. 1, art. 012052, 2021. <https://doi.org/10.1088/1757-899X/1094/1/012052>
- Gobierno Regional de Huánuco, *Política Ambiental y Climática 2021–2030*. Available: <https://www.regionhuanuco.gob.pe>
- F. Alberto *et al.*, "Water quality for irrigation in the Huallaga basin," *Scientia Agropecuaria*, vol. 13, no. 3, pp. 239–248, 2022. <https://doi.org/10.17268/sci.agropecu.2022.022>
- B. Laurence and W. Ronald, "Avoiding water hammer and other hydraulic transients," *Process Safety Progress*, vol. 43, no. 1, pp. 101–112, 2024. <https://doi.org/10.1002/prs.12517>
- R. Al-Khayat *et al.*, "Water hammer phenomenon in pumping stations," *Open Engineering*, vol. 12, no. 1, pp. 254–262, 2022. <https://doi.org/10.1515/eng-2022-0029>
- C. Huade, M. Magdi, and N. Ioan, "Finite element dynamic analysis of pipes subjected to water hammer," *Journal of Fluids and Structures*, vol. 93, art. 102845, 2020. <https://doi.org/10.1016/j.jfluidstructs.2019.102845>
- A. Ahmed, W. Rania, and A. Talaat, "Influence of pipe diameter and material on water hammer," *Journal of Advanced Engineering Trends*, vol. 43, no. 2, pp. 117–124, 2024.
- K. Natalia, "Experimental studies on pipe material effects on water hammer," *Acta Scientiarum Polonorum*, vol. 18, no. 1, pp. 15–26, 2019. <https://doi.org/10.15576/ASP.FC/2019.18.1.15>
- K. Rahul and K. Arun, "Experimental and numerical investigation of water hammer in pipelines," *International Journal of Pressure Vessels and Piping*, vol. 188, art. 104219, 2020. <https://doi.org/10.1016/j.ijpvp.2020.104219>
- M. Kubrak, "Water hammer mitigation by internal rubber hose," *Archives of Civil Engineering*, vol. 70, no. 1, pp. 275–288, 2024. <https://doi.org/10.24425/ace.2024.148911>
- Y. Jiawei *et al.*, "Optimization of pump turbine closing operation to minimize water hammer," *Energies*, vol. 13, no. 4, art. 1000, 2020. <https://doi.org/10.3390/en13041000>
- T. Abdelouaheb, S. Fateh, and A. Fateh, "Numerical modeling of water hammer using the MacCormack method," *Water Practice & Technology*, vol. 19, no. 6, pp. 2333–2351, 2024. <https://doi.org/10.2166/wpt.2024.138>
- K. Mehrdad *et al.*, "Comparison of CFD methods for modeling water hammer valve closure," *Water*, vol. 15, no. 8, art. 1510, 2023. <https://doi.org/10.3390/w15081510>
- Q. Lingxiao *et al.*, "Analysis of water hammer and pipeline vibration characteristics," *Journal of Marine Science and Engineering*, vol. 11, no. 10, art. 1885, 2023. <https://doi.org/10.3390/jmse11101885>

- A. Mohsen, R. Alireza, and T. Pedram, "Numerical analysis of fluid hammer in helical pipes," *International Journal of Pressure Vessels and Piping*, vol. 181, art. 104068, 2020. <https://doi.org/10.1016/j.ijpvp.2020.104068>
- P. Víctor, L. Jose, and M. Enrique, "Low-flow simulation modeling in South-Central Chile watersheds," *Water*, vol. 11, no. 7, art. 1506, 2019. <https://doi.org/10.3390/w11071506>